Chemical feedbacks weaken the wintertime response of particulate sulfate and nitrate to emissions reductions over the eastern United States

Viral Shah[a,1], Lyatt Jaeglé[a], Joel A. Thornton[a], Felipe D. Lopez-Hilfiker[a,2], Ben H. Lee[a], Jason C. Schroder[b,c], Pedro Campuzano-Jost[b,c], Jose L. Jimenez[b,c], Hongyu Guo[d], Amy P. Sullivan[e], Rodney J. Weber[d], Jaime R. Green[f], Marc N. Fiddler[g], Solomon Bililign[g,h], Teresa L. Campos[i,j], Meghan Stell[j,3], Andrew J. Weinheimer[i], Denise D. Montzka[i], and Steven S. Brown[b,k]

[a]Department of Atmospheric Sciences, University of Washington, Seattle, WA 98195; [b]Department of Chemistry, University of Colorado Boulder, Boulder, CO 80309; [c]Cooperative Institute for Research in Environmental Sciences (CIRES), University of Colorado Boulder, Boulder, CO 80309; [d]School of Earth and Atmospheric Sciences, Georgia Institute of Technology, Atlanta, GA 30332; [e]Department of Atmospheric Science, Colorado State University, Fort Collins, CO 80523; [f]Department of Energy and Environmental Systems, North Carolina A&T State University, Greensboro, NC 27411; [g]National Oceanic and Atmospheric Administration (NOAA) Interdisciplinary Scientific Environmental Technology (ISET) Cooperative Science Center, North Carolina A&T State University, Greensboro, NC 27411; [h]Department of Physics, North Carolina A&T State University, Greensboro, NC 27411; [i]Atmospheric Chemistry Observations and Modeling Laboratory, National Center for Atmospheric Research, Boulder, CO 80305; [j]Earth Observing Laboratory, National Center for Atmospheric Research, Boulder, CO 80305; and [k]Chemical Sciences Division, Earth System Research Laboratory, NOAA, Boulder, CO 80305

Edited by Mark H. Thiemens, University of California, San Diego, La Jolla, CA, and approved June 19, 2018 (received for review February 22, 2018)

Sulfate (SO_4^{2-}) and nitrate (NO_3^-) account for half of the fine particulate matter mass over the eastern United States. Their wintertime concentrations have changed little in the past decade despite considerable precursor emissions reductions. The reasons for this have remained unclear because detailed observations to constrain the wintertime gas–particle chemical system have been lacking. We use extensive airborne observations over the eastern United States from the 2015 Wintertime Investigation of Transport, Emissions, and Reactivity (WINTER) campaign; ground-based observations; and the GEOS-Chem chemical transport model to determine the controls on winter SO_4^{2-} and NO_3^-. GEOS-Chem reproduces observed SO_4^{2-}–NO_3^-–NH_4^+ particulate concentrations (2.45 μg sm^{-3}) and composition (SO_4^{2-}: 47%; NO_3^-: 32%; NH_4^+: 21%) during WINTER. Only 18% of SO_2 emissions were regionally oxidized to SO_4^{2-} during WINTER, limited by low [H_2O_2] and [OH]. Relatively acidic fine particulates (pH∼1.3) allow 45% of nitrate to partition to the particle phase. Using GEOS-Chem, we examine the impact of the 58% decrease in winter SO_2 emissions from 2007 to 2015 and find that the H_2O_2 limitation on SO_2 oxidation weakened, which increased the fraction of SO_2 emissions oxidizing to SO_4^{2-}. Simultaneously, NOx emissions decreased by 35%, but the modeled NO_3^- particle fraction increased as fine particle acidity decreased. These feedbacks resulted in a 40% decrease of modeled [SO_4^{2-}] and no change in [NO_3^-], as observed. Wintertime [SO_4^{2-}] and [NO_3^-] are expected to change slowly between 2015 and 2023, unless SO_2 and NOx emissions decrease faster in the future than in the recent past.

sulfate | nitrate | winter | anthropogenic emissions | $PM_{2.5}$

The past decade has seen dramatic reductions of sulfur dioxide (SO_2) and nitrogen oxides (NOx) emissions from power plants and vehicles in the United States (1, 2). Thus, hundreds of thousands of deaths and illnesses from exposure to fine particulate matter of aerodynamic diameter less than 2.5 μm ($PM_{2.5}$) have been averted (3). Between 2007 and 2015, annual SO_2 and NOx emissions in the United States have decreased by 68% and 36%, respectively (1). SO_2 and NOx are precursors of sulfate (SO_4^{2-}) and particulate nitrate (NO_3^-)—two major constituents of $PM_{2.5}$ in the eastern United States (4). Ground-based observations show that in response to these decreases in precursor emissions, annual average $PM_{2.5}$ concentrations in the eastern United States have decreased by a third between 2007 and 2015 (5). However, this decrease in $PM_{2.5}$ has occurred mostly in summer; $PM_{2.5}$ decreased only half as much in winter as in summer (1, 6). A similar seasonal difference in the $PM_{2.5}$ response to emission reductions has occurred in Western Europe too (6, 7). Severe wintertime $PM_{2.5}$ pollution is prevalent in eastern China and northern India (8, 9) and has led to strong mitigation measures. The design of effective strategies for air-quality improvement in the United States and many other countries critically depends on a process-based understanding of the response of wintertime $PM_{2.5}$ to emission reductions.

A closer examination of the $PM_{2.5}$ composition observed at the US Environmental Protection Agency (EPA) monitoring sites in the eastern United States illustrates the stark seasonal differences in [SO_4^{2-}] and [NO_3^-] changes between 2007 and 2015 (Fig. 1*A* and *SI Appendix*, Fig. S1). [The eastern United States

Significance

Exposure to fine particulate matter is a leading cause of premature deaths and illnesses globally. In the eastern United States, substantial cuts in sulfur dioxide and nitrogen oxides emissions have considerably lowered particulate sulfate and nitrate concentrations for all seasons except winter. Simulations that reproduce detailed airborne observations of wintertime atmospheric chemistry over the eastern United States indicate that particulate sulfate and nitrate formation is limited by the availability of oxidants and by the acidity of fine particles, respectively. These limitations relax at lower ambient concentrations, forming particulate matter more efficiently, and weaken the effect of emission reductions. These results imply that larger emission reductions, especially during winter, are necessary for substantial improvements in wintertime air quality in the eastern United States.

Author contributions: L.J., J.A.T., J.L.J., R.J.W., and S.S.B. designed research; V.S., L.J., J.A.T., F.D.L.-H., B.H.L., J.C.S., P.C.-J., J.L.J., H.G., A.P.S., R.J.W., J.R.G., M.N.F., S.B., T.L.C., M.S., A.J.W., D.D.M., and S.S.B. performed research; V.S., L.J., J.C.S., P.C.-J., and J.L.J. analyzed data; and V.S., L.J., J.A.T., J.C.S., P.C.-J., J.L.J., A.P.S., R.J.W., and S.S.B. wrote the paper.

The authors declare no conflict of interest.

This article is a PNAS Direct Submission.

Data deposition: The WINTER HR-ToF-AMS measurement data are available at the National Center for Atmospheric Research Earth Observing Laboratory (EOL) data archive (https://doi.org/10.5065/D6HX19V6), and the GEOS-Chem simulation results are available at the University of Washington data archive (http://hdl.handle.net/1773/41973).

[1]To whom correspondence should be addressed. Email: vshah@uw.edu.

[2]Present address: TOFWERK AG, CH-3600 Thun, Switzerland.

[3]Present address: Undergraduate Research Opportunities Center, California State University, Monterey Bay, CA 93955.

This article contains supporting information online at www.pnas.org/lookup/suppl/doi:10.1073/pnas.1803295115/-/DCSupplemental.

Published online July 23, 2018.

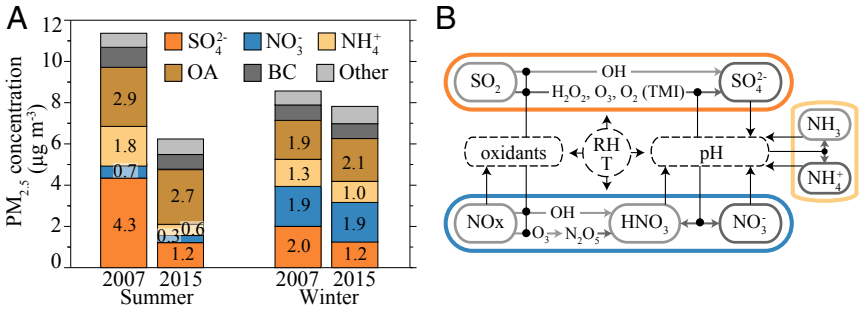

Fig. 1. $PM_{2.5}$ concentration change and SO_4^{2-}, NO_3^-, and NH_4^+ wintertime chemistry. (*A*) Population-weighted $PM_{2.5}$ concentration and composition observed over the eastern United States for summer (July, August, and September) and winter (January, February, and March) of 2007 and 2015. The $PM_{2.5}$ composition is separated into sulfate (SO_4^{2-}), nitrate (NO_3^-), ammonium (NH_4^+), organic aerosol (OA), black carbon (BC), and sea-salt and crustal material (Other). $PM_{2.5}$ observations are from 59 EPA $PM_{2.5}$ monitoring stations (*SI Appendix*, Fig. S1). In 2007–2015, annual SO_2 and NOx emissions in the United States decreased by 68% and 36%, respectively (1). (*B*) A representation of the important interactions in the wintertime chemistry of SO_4^{2-}, NO_3^-, NH_4^+, and their precursors.

is defined here as 31–43°N, 67–86.5°W (*SI Appendix*, Fig. S1*A*) and [...] denotes atmospheric concentration; that is, amount of the chemical constituent in a unit volume of air.] During this time, average summertime [SO_4^{2-}] and [NO_3^-] decreased by 72% and 50%, respectively, with an associated 67% decrease in ammonium (NH_4^+) concentrations. In contrast, wintertime [SO_4^{2-}] decreased by only 40%, [NH_4^+] by 23%, and [NO_3^-] did not change (Fig. 1*A*). These wintertime trends in SO_4^{2-}–NO_3^-–NH_4^+ $PM_{2.5}$ have been unfolding since 1990 (10), but a robust explanation for this weak response has been elusive.

During winter, the formation of SO_4^{2-}–NO_3^-–NH_4^+ $PM_{2.5}$ from emitted precursors is governed by strong feedbacks associated with oxidant availability, cloud water chemistry, and gas–particle partitioning (Fig. 1*B*). Due to lower concentrations of gas-phase photochemical oxidants during winter, SO_4^{2-} is formed mostly through aqueous-phase oxidation of SO_2 via reactions with hydrogen peroxide (H_2O_2), ozone (O_3), and oxygen (O_2) in clouds. The SO_2–O_2 reaction is catalyzed by transition metal ions (TMIs). Particulate NO_3^- and particulate NH_4^+ are in equilibrium with nitric acid (HNO_3) and ammonia (NH_3) gases, respectively. Particulate NO_3^- and NH_4^+ are favored at low temperature and high relative humidity (RH). During winter, HNO_3 formation by hydrolysis of dinitrogen pentoxide (N_2O_5) on aqueous particles becomes more important than by reaction of nitrogen dioxide (NO_2) with hydroxyl radicals (OH). NOx concentrations themselves, in turn, control oxidant concentrations, which influence SO_2 to SO_4^{2-} oxidation rates. In-cloud SO_2 oxidation by O_3 becomes faster with increasing pH. Similarly, the fraction of HNO_3 forming particulate NO_3^- increases with increasing fine-particle pH (11, 12). Most of the NH_3 gas partitions to particulate NH_4^+ at pH below 3, which is typical for fine particles in the eastern United States. The pH of fine particles and cloud water depends on the overall gas and particle composition (Fig. 1*B*). In the eastern United States during winter, fine-particle pH increases with increasing [NH_3] and decreases as [SO_4^{2-}] increases but is less sensitive to changes in [HNO_3] and [NO_3^-] (13).

The state of this chemical system and its feedbacks determine the response of [SO_4^{2-}] and [NO_3^-] to emission reductions. However, reproducing the observed concentrations and trends has been a challenge for current atmospheric chemical transport models. Models are largely unable to reproduce observed wintertime concentrations, particularly of NO_3^- (14–16), and fail to capture wintertime trends in [SO_4^{2-}] and [NO_3^-] (6, 17), resulting in unclear policy guidance. Explanations for the weak response of [SO_4^{2-}] to emission reductions include higher SO_2 oxidation efficiency because of a weakening H_2O_2 limitation on the SO_2–H_2O_2 reaction (17, 18), rising cloud water pH (17), and higher [OH] and [H_2O_2] with lower NOx emissions (18, 19). Some modeling studies have suggested that NO_3^- formation in the eastern United States is limited by the availability of NH_3, such that [NO_3^-] is weakly sensitive to [HNO_3] but increases as [SO_4^{2-}] is lowered and NH_3 availability increases (18–21).

A lack of detailed observations of SO_4^{2-}–NO_3^-–NH_4^+ $PM_{2.5}$ and particularly of their precursors during winter has impeded verification of these various hypotheses. The 2015 Wintertime Investigation of Transport, Emissions, and Reactivity (WINTER) aircraft campaign has produced a unique set of comprehensive atmospheric composition observations over the eastern United States. Here, we use the GEOS-Chem chemical transport model, evaluated against airborne WINTER observations and ground-based observations, to show that the formation of SO_4^{2-} and NO_3^- $PM_{2.5}$ in winter is controlled by OH- and H_2O_2-mediated SO_2 oxidation and by fine-particle pH, respectively. We demonstrate that the weakening H_2O_2 limitation and increasing fine-particle pH have caused the weak response of [SO_4^{2-}] and [NO_3^-] to emission reductions.

Observations and Simulation Results for Winter 2015

The WINTER campaign consisted of 13 daytime and nighttime flights between February 1 and March 15, 2015 (*SI Appendix*, Fig. S2) on the US National Science Foundation (NSF)/National Center for Atmospheric Research (NCAR) C-130 aircraft equipped with a detailed payload to measure gas and particle concentrations. The majority (71%) of the measurements were made below an altitude of 1 km. Concentrations of nonrefractory SO_4^{2-}–NO_3^-–NH_4^+ PM_1 (PM with aerodynamic diameter <1 μm) were made with a high-resolution time-of-flight aerosol mass spectrometer (HR-ToF-AMS; Aerodyne Research Inc.) (22, 23). SO_2 was measured by pulsed UV fluorescence (Thermo Electron Corporation) and HNO_3 with the Iodide-adduct high-resolution time-of-flight chemical ionization mass spectrometer (HRToF-CIMS) (24). Other instruments onboard measured carbon monoxide (CO), O_3, reactive nitrogen (NOy), and meteorological variables. These measurements were used to fully evaluate the GEOS-Chem model (*SI Appendix*, Fig. S3).

In the following analysis, we assume that the PM_1 mass composition is representative of that of $PM_{2.5}$ for SO_4^{2-}–NO_3^-–NH_4^+ over land and that the influence of other ions (such as Na^+, Ca^{2+}, or Cl^-) on the chemistry of SO_4^{2-}–NO_3^-–NH_4^+ $PM_{2.5}$ is negligible. SO_4^{2-} and NO_3^- are present on coarse (diameter >1 μm) sea-salt and dust particles, but sea salt and dust are minor components of the $PM_{2.5}$ over the eastern United States (Fig. 1*A*) and, when present, are typically externally mixed with SO_4^{2-}–NO_3^-–NH_4^+ PM_1 (25). Guo et al. (12) showed that during WINTER nearly all SO_4^{2-} and NO_3^- over land is present as PM_1 and that excluding the other ions in thermodynamic calculations results in better agreement with the observations. Therefore, hereafter, SO_4^{2-}–NO_3^-–NH_4^+ refers to those components in PM_1.

The observed horizontal and vertical distributions of SO_4^{2-}–NO_3^-–NH_4^+ are reproduced by the GEOS-Chem model (Fig. 2). Below 1 km altitude, mean observed SO_4^{2-}–NO_3^-–NH_4^+ during WINTER was 2.45 μg·sm^{-3} (1 sm^3 is 1 m^3 at 273.15 K and 1,013.25 hPa), with higher concentrations downwind of the

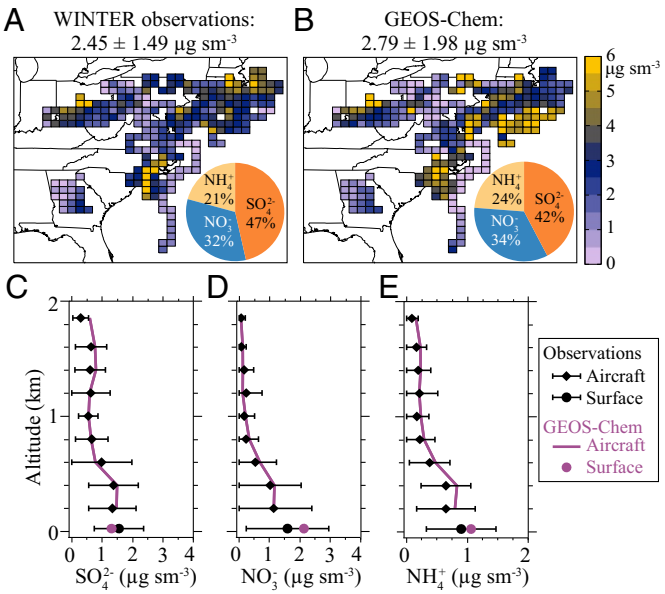

Fig. 2. Spatial distribution of (*A*) observed and (*B*) GEOS-Chem concentrations of SO_4^{2-}–NO_3^-–NH_4^+ PM_1 along the WINTER flight paths (February 1–March 15, 2015) below 1 km altitude (in units of μg·sm^{-3}, where 1 sm^3 equals 1 m^3 at 273.15 K and 1013.25 hPa). The observations are gridded onto the 0.5° latitude by 0.625° longitude GEOS-Chem grid. The number of 1-min average observations in each grid box varies from 1 to 79, with a median of 10 observations. The WINTER campaign means ± standard deviations (SD) are shown above *A* and *B*. The *Inset* pie charts show the corresponding mean composition of PM_1. Also shown are the mean vertical profiles of observed (black diamonds and error bars: mean ± SD for each altitude bin) and GEOS-Chem (purple line) concentrations of (*C*) SO_4^{2-}, (*D*) NO_3^-, and (*E*) NH_4^+ along the WINTER flight tracks. Also shown are the mean observations for the ground-based CSN, IMPROVE, and CASTNET networks (black filled circles with SD) and corresponding model results (purple filled circles) for February 1–March 15, 2015.

source regions in the Northeast Urban Corridor and in the Ohio River Valley (Fig. 2*A*). GEOS-Chem predicts mean concentrations (2.79 μg·sm^{-3}) and spatial patterns consistent with the observations (Fig. 2*B*). Furthermore, the observed composition of SO_4^{2-}–NO_3^-–NH_4^+ (47% SO_4^{2-}; 32% NO_3^-; 21% NH_4^+) is reproduced by GEOS-Chem (42% SO_4^{2-}; 34% NO_3^-; 24% NH_4^+). GEOS-Chem results are also in agreement with the ground-based observations at the Chemical Speciation Network (CSN), the Interagency Monitoring of Protected Visual Environments (IMPROVE) network, and the Clean Air Status and Trends Network (CASTNET) for February 1–March 15, 2015 (*SI Appendix*, Fig. S4 *A* and *B*). The ability of GEOS-Chem to simulate the wintertime SO_4^{2-}–NO_3^-–NH_4^+ over the eastern United States is further demonstrated by the agreement between the simulated and observed vertical profiles of [SO_4^{2-}], [NO_3^-], [NH_4^+] (Fig. 2 *C*–*E*), [SO_2], and [HNO_3] (*SI Appendix*, Fig. S5).

Past studies have found that GEOS-Chem simulations overestimate wintertime [NO_3^-] over the eastern United States by a factor of 3 (15, 19)—an issue common to many models (14, 16). The WINTER observations have allowed a detailed analysis of nighttime and daytime NOx chemistry, HNO_3 formation, and HNO_3 dry deposition, leading to improvements in the representation of these processes in GEOS-Chem and a substantial reduction of the [NO_3^-] overestimate. In particular, we have updated the dry deposition velocities for winter conditions and assume that for HNO_3 the resistance to surface uptake is negligible, resulting in faster deposition of HNO_3 and other gas species (*SI Appendix*, *Section 1.1*). We have also updated the calculation of the reactive uptake probability of N_2O_5 on particles based on recent laboratory studies, resulting in slower conversion of NOx to HNO_3 (*SI Appendix*, *Section 1.2*).

Having evaluated the consistency of the GEOS-Chem results with aircraft and ground-based observations, we now explore how wintertime SO_4^{2-} and NO_3^- are formed.

Processes Controlling the Formation of SO_4^{2-} and NO_3^- in Winter

Gas-phase and in-cloud oxidation of SO_2 to SO_4^{2-} account for 90% of the modeled SO_4^{2-} source below 2 km altitude in the eastern United States during WINTER, with primary anthropogenic emissions of SO_4^{2-} accounting for the remaining 10%. We use GEOS-Chem to determine the SO_2 to SO_4^{2-} oxidation efficiency [$\eta(SO_4^{2-})$]:

$$\eta(SO_4^{2-}) = \frac{SO_2 \text{ mass oxidized below 2 km (kg d}^{-1})}{SO_2 \text{ mass emitted (kg d}^{-1})}. \quad [1]$$

We calculate that over the eastern United States during WINTER $\eta(SO_4^{2-})$ = 0.18. In GEOS-Chem, we find that 46% of SO_2 oxidation is due to reaction with H_2O_2 in cloud water, 35% due to gas-phase reaction with OH, and the rest due to in-cloud SO_2–O_3 and the TMI-catalyzed pathways. The slow winter photochemistry results in low [H_2O_2] (GEOS-Chem winter [H_2O_2] is 0.2 ppbv, 10-fold lower than summer) and [OH]. While recent work suggests higher oxidant concentrations in winter than previously expected (26, 27), these oxidant sources are not large enough to shift the relationship between H_2O_2 and SO_2 (*SI Appendix*, *Section 2*). SO_2 oxidation during winter is limited by the availability of H_2O_2, which can be entirely consumed in the SO_2–H_2O_2 reaction. Fig. 3*A* illustrates the relationship in GEOS-Chem between the [H_2O_2]/[SO_2] ratio and the oxidation rate of SO_2 to SO_4^{2-} by reaction with H_2O_2 ($R_{SO_2-H_2O_2}$), defined here as:

$$R_{SO_2-H_2O_2} = \frac{SO_2 \text{ mass oxidized by } H_2O_2 \text{ below 2 km (kg d}^{-1})}{SO_2 \text{ mass present below 2 km (kg)}}. \quad [2]$$

The winter H_2O_2 limitation is demonstrated by the increase of $R_{SO_2-H_2O_2}$ to around 0.35 d^{-1} as [H_2O_2]/[SO_2] increases to 3, beyond which $R_{SO_2-H_2O_2}$ becomes independent of this ratio and no longer H_2O_2-limited (Fig. 3*A*). Part of the variability in $R_{SO_2-H_2O_2}$ is due to local variability in cloud liquid water content. The lower troposphere over land in the eastern United States lies in the H_2O_2-limited regime (mean [H_2O_2]/[SO_2] = 0.4). The modeled [H_2O_2]/[SO_2] ratio increases over the ocean as [SO_2] decreases away from source regions and [H_2O_2] increases southward with stronger photochemical production.

Particle-phase NO_3^- is in equilibrium with gas-phase HNO_3 [$HNO_3(g) \leftrightarrow H^+ + NO_3^-$]. This equilibrium shifts to the particle phase at colder temperatures and at higher particle pH. Fig. 3*B* shows how the GEOS-Chem nitrate particle fraction ($\epsilon(NO_3^-) = \frac{[NO_3^-]}{[HNO_3]+[NO_3^-]}$) varies as a function of modeled PM_1 pH and temperature during WINTER below 1 km altitude. The WINTER campaign observations of $\epsilon(NO_3^-)$ and PM_1 pH inferred from thermodynamic analysis of observed PM_1 composition (shown as gray circles in Fig. 3*B*) confirm this pattern of increasing $\epsilon(NO_3^-)$ with increasing PM_1 pH (12). During WINTER, the GEOS-Chem predicted median PM_1 pH over land below 1 km altitude was 1.29 and $\epsilon(NO_3^-)$ was 0.45, in good agreement with those inferred from the measurements (pH = 1.34 and $\epsilon(NO_3^-)$ = 0.48 for RH > 40%) (12). Local variations in PM_1 pH and temperature influence the variability in $\epsilon(NO_3^-)$ in the model, with larger $\epsilon(NO_3^-)$ (>0.7) simulated over the colder Midwest with high PM_1 pH (~2) owing to higher NH_3 and lower SO_2 emissions and smaller $\epsilon(NO_3^-)$ (<0.4) simulated off the East Coast over the warmer ocean and with lower PM_1

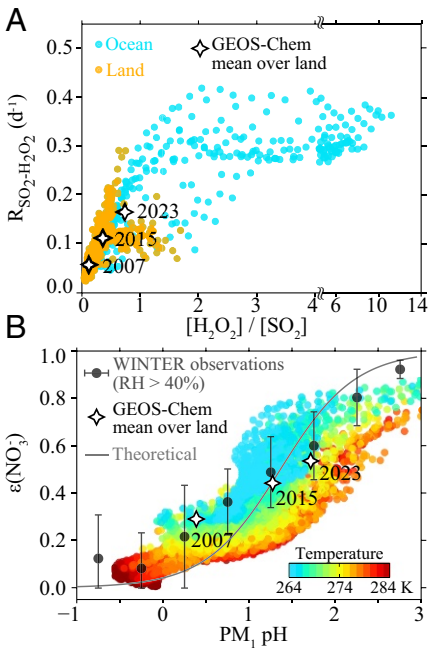

Fig. 3. Factors controlling wintertime SO_4^{2-} and NO_3^- formation. (*A*) GEOS-Chem simulated relationship between the oxidation rate of SO_2 to SO_4^{2-} by reaction with H_2O_2 ($R_{SO_2-H_2O_2}$) and the H_2O_2/SO_2 concentration ratio for February 1–March 15, 2015 in the bottom 2 km over the eastern United States (31–43°N, 67 to 86.5°W). The stars represent the mean $R_{SO_2-H_2O_2}$ and H_2O_2/SO_2 ratio over land in the eastern United States for the 2007, 2015, and 2023 simulations. The 2007–2015 change in wintertime SO_2 and NOx emissions is −58% and −35%, respectively, and the 2015–2023 change is −47% and −25%. (*B*) GEOS-Chem simulated fraction of nitrate in the particle phase [$\epsilon(NO_3^-)$] as a function of PM_1 pH and temperature in the bottom 1 km over the eastern United States. Dark gray circles and error bars represent the measured $\epsilon(NO_3^-)$ (means ± SD) as a function of the measurement-inferred PM_1 pH for WINTER observations below 1 km altitude (12). Only observations with RH >40% are considered. The stars are the mean $\epsilon(NO_3^-)$ and PM_1 pH in the bottom 1 km over land in the eastern United States for the 2007, 2015, and 2023 simulations. The theoretical relationship between $\epsilon(NO_3^-)$ and PM_1 pH for the 2015 mean WINTER conditions is shown by the gray curve.

pH. Further away from the coast, sea-salt particles can mix with SO_4^{2-}–NO_3^-–NH_4^+ and influence the pH.

The WINTER observations provide constraints for the simulated values of $\eta(SO_4^{2-})$, PM_1 pH, and $\epsilon(NO_3^-)$—the parameters controlling the formation of winter SO_4^{2-} and NO_3^-. There were no WINTER measurements of [OH], [H_2O_2], and cloud water pH, adding uncertainty to our calculated contributions of the different SO_2 oxidation pathways to $\eta(SO_4^{2-})$. However, we find good agreement between GEOS-Chem and the WINTER observations of OH and H_2O_2 precursors (*SI Appendix*, Fig. S3), which provides indirect constraints on the simulated [OH] and [H_2O_2]. Moreover, we find that the GEOS-Chem results are weakly sensitive to uncertainties in the simulated [OH] and [H_2O_2] (*SI Appendix*, *Section 2*). A 50% increase in modeled [H_2O_2] increases $R_{SO_2-H_2O_2}$ by 37%, and SO_4^{2-} formation remains H_2O_2-limited. The resulting increase in [SO_4^{2-}] is less than 5% because of compensating effects by other oxidation pathways. Our results are somewhat more sensitive to uncertainties in NH_3 emissions (via PM_1 pH; *SI Appendix*, *Section 2.3*), which have few observational constraints on their magnitude and seasonality. We estimate an uncertainty in our simulated PM_1 pH of ∼0.3 units because of the uncertainty in NH_3 emissions and a similar uncertainty due to neglecting the influence of Na^+ cations (12). A change in PM_1 pH of 0.3 units changes the simulated [NO_3^-] for WINTER by ∼30% and does not alter the dependence of $\epsilon(NO_3^-)$ on PM_1 pH.

Response of Winter [SO_4^{2-}] and [NO_3^-] to Emissions Reductions

We now turn to explaining the weak response of wintertime [SO_4^{2-}] and [NO_3^-] to decreases in SO_2 and NOx emissions between 2007 and 2015 and examining the future response of [SO_4^{2-}] and [NO_3^-] under the 2023 EPA emissions projections (28). To address these issues, we have performed additional GEOS-Chem simulations for February 1–March 15 with varying US SO_2 and NOx anthropogenic emissions: (*i*) a simulation with 2007 emissions of SO_2 (15.8 GgS·d^{-1}) and NOx (11.8 GgN·d^{-1}) (29), and (*ii*) a simulation with 2023 EPA projected emissions of SO_2 (3.5 GgS·d^{-1}) and NOx (5.8 GgN·d^{-1}) (29). Anthropogenic US emissions of SO_2 and NOx in 2015 were 6.6 GgS·d^{-1} and 7.7 GgN·d^{-1}, respectively (*SI Appendix*, Table S1). Meteorology can affect the interannual variability of $PM_{2.5}$ (30); therefore, to isolate the effect of SO_2 and NOx emissions reductions, we have used the same meteorological fields as for our 2015 simulation. Furthermore, our simulations do not include the EPA estimated 2007–2015 emission changes for other species, including NH_3 (−2%), CO (−30%), and volatile organic compounds (−14%) (29). Despite these simplifying assumptions, the 2007 simulation is consistent with ground-based $PM_{2.5}$ observations for February 1–March 15, 2007 (*SI Appendix*, Fig. S4 *C* and *D*).

Simulated surface [SO_4^{2-}] for February 1–March 15, 2015 is higher near SO_2 source regions in the Ohio River Valley (*SI Appendix*, Fig. S6) but display little spatial variation elsewhere (Fig. 4*A*). The regional extent of SO_4^{2-} pollution reflects the slow oxidation of SO_2 as it is transported downwind of its sources. Between 2007 and 2015, simulated [SO_4^{2-}] decreased everywhere in response to lower SO_2 emissions and continues to decrease between 2015 and 2023 (Fig. 4*A* and *SI Appendix*, Fig. S7 *A*–*C*). The 2007–2015 [SO_4^{2-}] decrease observed at surface sites (−0.83 μg·sm^{-3}; −31%) is reproduced by GEOS-Chem (−1.06 μg·sm^{-3}; −40%). Between 2015 and 2023, the mean modeled [SO_4^{2-}] at surface sites is projected to decrease by another 0.38 μg·sm^{-3} (−24%) (Fig. 5*A*).

The decrease in modeled [SO_4^{2-}] (2007–2015: −40%; 2015–2023: −24%) is significantly lower than the decrease in US SO_2 emissions (2007–2015: −58%; 2015–2023: −47%). This subdued response to emissions reductions is caused by a corresponding increase in $\eta(SO_4^{2-})$, from 0.11 (2007) to 0.18 (2015) and 0.26 (2023) (Fig. 5*B*), which counteracts the effect of reduced SO_2 emissions by allowing a larger fraction of the emissions to be oxidized to SO_4^{2-} on regional and local scales. In the model, the increase in $\eta(SO_4^{2-})$ is driven by the SO_2–H_2O_2 pathway (Fig. 5*B*): Reduced SO_2 concentrations lead to a factor of 2.7 increase in the [H_2O_2]/[SO_2] ratio between 2007 and 2015 and another factor of 2 increase between 2015 and 2023, thereby lowering the degree of H_2O_2 limitation (Fig. 3*A*). The [H_2O_2]/[SO_2] ratio increases mostly because of the decrease in SO_2 concentrations

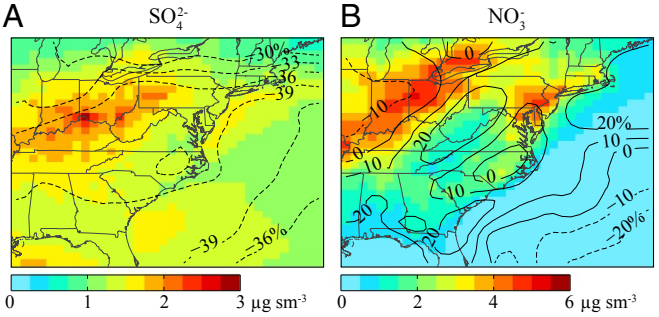

Fig. 4. GEOS-Chem surface concentrations of (*A*) SO_4^{2-} and (*B*) NO_3^- PM_1 for February 1–March 15, 2015. The contour lines show the percent change relative to February 1–March 15, 2007 concentrations $100 \times \left(\frac{[2015]-[2007]}{[2007]}\right)$.

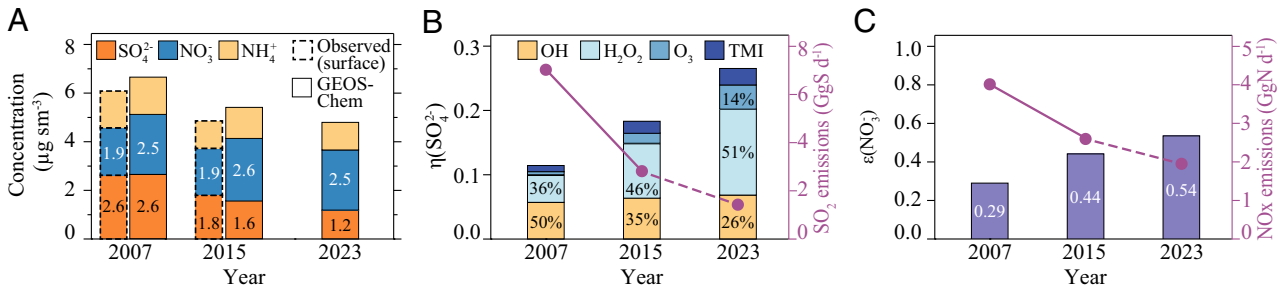

Fig. 5. Past and future changes in wintertime SO_4^{2-}–NO_3^-–NH_4^+ concentration and formation efficiency. (*A*) Average surface concentrations of SO_4^{2-}–NO_3^-–NH_4^+ $PM_{2.5}$ for the eastern United States for February 1–March 15, 2007, 2015, and 2023 simulated by GEOS-Chem and observed at the ground-based sites (2007 and 2015, bars with dashed lines). (*B*) SO_2 to SO_4^{2-} oxidation efficiency $\eta(SO_4^{2-})$ over land partitioned by pathway: gas-phase oxidation with OH, aqueous oxidation with H_2O_2, O_3, and O_2 catalyzed by TMIs. SO_2 emissions over the eastern United States are shown (in purple) for the three simulations. (*C*) Fraction of nitrate in the particle phase ($\epsilon(NO_3^-)$) and NOx emissions (in purple) over land in the eastern United States for the three simulations.

and, to a small extent, because of higher $[H_2O_2]$ at lower NOx emissions. A small increase in $\eta(SO_4^{2-})$ is also caused by a faster rate of the SO_2–O_3 aqueous reaction with increasing cloud water pH at lower SO_2 emissions (Fig. 5*B*). In our simulations, mean cloud water pH over the eastern United States rises from 4.2 (2007) to 4.6 (2023). Our results suggest that beyond 2023, $\eta(SO_4^{2-})$ will continue to increase with continued relaxation of the H_2O_2 limitation and rise in cloud water pH, further weakening the response of $[SO_4^{2-}]$ to emission reductions. Beyond 2023, rising cloud water pH could become a more important factor in the continued increase in $\eta(SO_4^{2-})$ and drive wintertime $\eta(SO_4^{2-})$ to above 0.5 by 2050 (17).

The model reproduces the observed lack of change in $[NO_3^-]$ over the region between 2007 and 2015, despite a 35% reduction in NOx emissions (Figs. 4*B* and 5*A* and *SI Appendix*, Fig. S7 *D* and *E*). We calculate that the additional 25% decrease in NOx emissions expected by 2023 will not produce much change in $[NO_3^-]$ (Fig. 5*A* and *SI Appendix*, Fig. S6*F*). We find that the production of total (gas + particle) nitrate in the model decreases linearly with decreasing NOx emissions. But this decrease in nitrate formation is counteracted by an increase in $\epsilon(NO_3^-)$, buffering the response of $[NO_3^-]$ (Fig. 5*C*). In addition, the shift of nitrate to the particle phase increases its lifetime [as NO_3^- deposits at a slower rate than HNO_3 (31)] and further offsets the decrease in total nitrate production. Between 2007 and 2023, modeled $\epsilon(NO_3^-)$ nearly doubles (0.29 to 0.54), canceling the expected effect of NOx emissions reduction. The increase in $\epsilon(NO_3^-)$ is caused by an increase in PM_1 pH from 0.39 to 1.7 (2007–2023) (Fig. 3*B*) mainly because of decreasing $[SO_4^{2-}]$ and, to a smaller extent, $[HNO_3]$ but also because of the positive feedback between $\epsilon(NO_3^-)$ and PM_1 pH due to the hygroscopicity of NO_3^- (32). There are local differences in the balance between increasing PM_1 pH and decreasing NOx emissions. For example, $[NO_3^-]$ increases downwind of the Ohio River Valley, where the increase in PM_1 pH outpaces the decrease in NOx emissions (Fig. 4*B* and *SI Appendix*, Fig. S7 *D*–*F*).

It is important to note that if the 2007–2015 decrease in SO_2 emissions had not been accompanied by a decrease in NOx emissions, the result would have been a 30% increase in $[NO_3^-]$ over the eastern United States, in response to decreasing $[SO_4^{2-}]$ and hence rising PM_1 pH and $\epsilon(NO_3^-)$. It was purely coincidental that the increase in $\epsilon(NO_3^-)$, driven largely by the decrease in SO_2 emissions, was closely matched by the decrease in NOx emissions, preventing such a regional increase in $[NO_3^-]$. A similar trend is expected to continue until 2023 (Fig. 5 *A* and *C*). At some point beyond 2023, as PM_1 pH increases, $\epsilon(NO_3^-)$ will approach 1, and $[NO_3^-]$ will start responding more linearly to NOx emission reductions. Our simulations suggest that winter $[NO_3^-]$ will not decrease much in response to future NOx emissions reductions, unless the rate of winter NOx emission reductions exceeds the rate of increase in $\epsilon(NO_3^-)$.

The effectiveness of NOx emissions reductions will be further diminished if emissions of NH_3 were to increase. The EPA projects almost no change in US NH_3 emissions by 2023 (28), but these predictions are uncertain because of weak regulatory oversight on NH_3. PM_1 pH is sensitive to NH_3 under present winter conditions over the eastern United States (*SI Appendix*, *Section 2.3*). If NH_3 emissions were to increase in the future, PM_1 pH would increase, causing an increase in the conversion of NOx to $[NO_3^-]$ (due to $\epsilon(NO_3^-)$ increasing with pH). This response of PM_1 pH to NH_3 emissions is not necessarily true in other seasons and locations where both the PM_1 pH and the dependence of $\epsilon(NO_3^-)$ on pH may differ (11, 32).

Conclusions

Wintertime $[SO_4^{2-}]$ and $[NO_3^-]$ in the eastern United States have responded weakly to SO_2 and NOx emissions reductions. While previous modeling studies have examined the sensitivity of wintertime $[SO_4^{2-}]$ and $[NO_3^-]$ to emission reductions, the fidelity of these models could not be verified without the constraints of detailed in situ observations. In this study, we have presented aircraft observations of SO_4^{2-}–NO_3^-–NH_4^+ PM_1 concentrations and precursor gases that serve as crucial benchmarks for models. We have shown that the GEOS-Chem model simulation of SO_4^{2-}–NO_3^-–NH_4^+ PM_1 concentration and composition is in good agreement with the WINTER campaign observations. GEOS-Chem results for the WINTER campaign showed that 18% of the SO_2 is regionally oxidized to SO_4^{2-} in winter over the eastern United States, compared with about 35% during summer. In GEOS-Chem, SO_2 oxidation happens mostly by H_2O_2 (46%) and OH (35%) and is limited by low wintertime $[H_2O_2]$ and [OH]. The observations and model show that about 45% of the total nitrate (gas + particle) was in the particle phase during the WINTER campaign period because of low PM_1 pH (~1.3).

GEOS-Chem is able to reproduce the weak decrease in winter $[SO_4^{2-}]$ and $[NO_3^-]$ between 2007 and 2015 observed at ground-based sites. With our simulations, we find that as SO_2 and NOx emissions decrease, the resulting increase in $[H_2O_2]/[SO_2]$ and PM_1 pH leads to more efficient regional formation of SO_4^{2-} and NO_3^- per unit mass of precursor pollutant emitted during winter. We project that these chemical feedbacks will persist into the near future. Between 2015 and 2023, we predict a 24% decrease in winter $[SO_4^{2-}]$ and little to no change in winter $[NO_3^-]$ despite an expected 47% decrease in SO_2 emissions and 25% decrease in NOx emissions. We also find that without concurrent decreases in NOx emissions, the 2007–2015 SO_2 emissions decrease would have resulted in a 30% increase in regional $[NO_3^-]$ due to PM_1 pH increase and its control on the fraction of nitrate in the particle phase. Similarly, for the future, if only SO_2 emissions were to decrease by 2023 and NOx emissions remained at 2015 levels, regional $[NO_3^-]$ would increase by 12%. These counteracting chemical feedbacks necessitate stronger reductions of both

SO_2 and NOx emissions during winter for faster improvements in wintertime air quality.

Materials and Methods

PM_1 [SO_4^{2-}], [NO_3^-], and [NH_4^+] were measured by the HR-ToF-AMS (22, 23, 33–35). Air was sampled through a forward-facing inlet mounted under the aircraft. It passes through a pressure-controlled inlet, an aerodynamic focusing lens, and a high-vacuum region to the detection chamber, where nonrefractory species are flash vaporized at 600 °C and ionized with 70 eV electron impact ionization. The ions are orthogonally extracted and analyzed by ToF mass spectrometry. The data were corrected for relative ionization and collection efficiencies (23). One-minute measurements are used here. Detection limits were 57 ng·sm^{-3} (SO_4^{2-}), 30 ng·sm^{-3} (NO_3^-), and 5 ng·sm^{-3} (NH_4^+), and accuracy was 35% (23).

CSN, IMPROVE, and CASTNET are ground-based $PM_{2.5}$ monitoring networks (36, 37). CSN and IMPROVE report 24-h mean concentrations every third or sixth day. We include only sites that report every third day. CASTNET measurements are weekly averages. We exclude sites with less than 70% temporal coverage for February 1–March 15, 2015. The eastern United States had 26 such CSN sites in 2015 (21 in 2007), 27 IMPROVE sites in 2015 (26 in 2007), and 26 CASTNET sites in 2015 (33 in 2007). When calculating the 2007–2015 change in $PM_{2.5}$ concentrations, we include only those sites that were operational in both years (CSN: 16; IMPROVE: 23; CASTNET: 23).

GEOS-Chem is driven by assimilated meteorological fields from NASA GMAO's GEOS-5 FP system (38). We use GEOS-Chem v10-01 in a nested-grid configuration: 0.5° latitude × 0.625° longitude resolution over North America and 4°×5° elsewhere. Simulations were performed for February 1–March 15, 2015. The model is described in *SI Appendix*. Anthropogenic emissions over the United States are from the EPA's 2011v6.1 (for 2011) and 2011v6.3 (for 2023) modeling platforms for the 2011 National Emissions Inventory (28, 39). The 2011 US emissions were scaled to 2015 levels (scaling factors SO_2: 0.72; NOx: 0.80; NH_3: 1.0) based on the EPA emissions trend report (29) and the Air Markets Program Data (40). Livestock NH_3 emissions were recalculated for 2015 meteorology. The 2007 and 2023 SO_2 and NOx emissions were based on EPA estimates (28, 29).

ACKNOWLEDGMENTS. We thank all members of the WINTER team for their contributions during the field campaign and the agencies operating the CSN, IMPROVE, and CASTNET networks. We are grateful to the entire GEOS-Chem user community and the NSF/NCAR Research Aircraft Facility pilots and crew. The WINTER campaign was supported by NSF Grant AGS-1360745. J.C.S., P.C.-J., and J.L.J. were supported by NSF Grant AGS-1360834 and NASA Grant NNX15AT96G and H.G. and R.J.W. by NSF Grant AGS-1360730.

1. EPA (2017) *Our nation's air*. Available at https://gispub.epa.gov/air/trendsreport/2017/. Accessed October 2, 2017.
2. Krotkov NA, et al. (2016) Aura OMI observations of regional SO_2 and NO_2 pollution changes from 2005 to 2015. *Atmos Chem Phys* 16:4605–4629.
3. Cohen AJ, et al. (2017) Estimates and 25-year trends of the global burden of disease attributable to ambient air pollution: An analysis of data from the global burden of diseases study 2015. *Lancet* 389:1907–1918.
4. Hand JL, Schichtel BA, Pitchford M, Malm WC, Frank NH (2012) Seasonal composition of remote and urban fine particulate matter in the United States: Composition of remote and urban aerosols. *J Geophys Res Atmos* 117:D05209.
5. EPA (2017) *Particulate Matter (PM2.5) trends*. Available at https://www.epa.gov/air-trends/particulate-matter-pm25-trends. Accessed October 18, 2017.
6. Xing J, et al. (2015) Observations and modeling of air quality trends over 1990–2010 across the northern hemisphere: China, the United States and Europe. *Atmos Chem Phys* 15:2723–2747.
7. Tørseth K, et al. (2012) Introduction to the European Monitoring and Evaluation Programme (EMEP) and observed atmospheric composition change during 1972–2009. *Atmos Chem Phys* 12:5447–5481.
8. Huang RJ, et al. (2014) High secondary aerosol contribution to particulate pollution during haze events in China. *Nature* 514:218–222.
9. Dey S, Di Girolamo L (2011) A decade of change in aerosol properties over the Indian subcontinent: Seasonal aerosol trends over India. *Geophys Res Lett* 38:L14811.
10. Sickles JE, II, Shadwick DS (2015) Air quality and atmospheric deposition in the eastern US: 20 years of change. *Atmos Chem Phys* 15:173–197.
11. Weber RJ, Guo H, Russell AG, Nenes A (2016) High aerosol acidity despite declining atmospheric sulfate concentrations over the past 15 years. *Nat Geosci* 9:282–285.
12. Guo H, et al. (2016) Fine particle pH and the partitioning of nitric acid during winter in the northeastern United States: Particle pH and nitric acid partitioning. *J Geophys Res Atmos* 121:10355–10376.
13. Guo H, Weber RJ, Nenes A (2017) High levels of ammonia do not raise fine particle pH sufficiently to yield nitrogen oxide-dominated sulfate production. *Sci Rep* 7 12109.
14. Simon H, Baker KR, Phillips S (2012) Compilation and interpretation of photochemical model performance statistics published between 2006 and 2012. *Atmos Environ* 61:124–139.
15. Heald CL, et al. (2012) Atmospheric ammonia and particulate inorganic nitrogen over the United States. *Atmos Chem Phys* 12:10295–10312.
16. Colette A, et al. (2011) Air quality trends in Europe over the past decade: A first multi-model assessment. *Atmos Chem Phys* 11:11657–11678.
17. Paulot F, Fan S, Horowitz LW (2017) Contrasting seasonal responses of sulfate aerosols to declining SO_2 emissions in the Eastern U.S.: Implications for the efficacy of SO_2 emission controls. *Geophys Res Lett* 44:455–464.
18. Tsimpidi AP, Karydis VA, Pandis SN (2007) Response of inorganic fine particulate matter to emission changes of sulfur dioxide and ammonia: The eastern United States as a case study. *J Air Waste Manag Assoc* 57:1489–1498.
19. Holt J, Selin NE, Solomon S (2015) Changes in inorganic fine particulate matter sensitivities to precursors due to large-scale US emissions reductions. *Environ Sci Technol* 49:4834–4841.
20. Park RJ, et al. (2004) Natural and transboundary pollution influences on sulfate-nitrate-ammonium aerosols in the United States: Implications for policy. *J Geophys Res Atmos* 109:D15204.
21. Pye HOT, et al. (2009) Effect of changes in climate and emissions on future sulfate-nitrate-ammonium aerosol levels in the United States. *J Geophys Res Atmos* 114:D01205.
22. DeCarlo PF, et al. (2006) Field-deployable, high-resolution, time-of-flight aerosol mass spectrometer. *Anal Chem* 78:8281–8289.
23. Schroder JC, et al. (2018) Sources and secondary production of organic aerosols in the Northeastern US during WINTER. *J Geophys Res Atmos*, 10.1029/2018JD028475.
24. Lee BH, et al. (2014) An iodide-adduct high-resolution time-of-flight Chemical-Ionization Mass Spectrometer: Application to atmospheric inorganic and organic compounds. *Environ Sci Technol* 48:6309–6317.
25. Middlebrook AM, et al. (2003) A comparison of particle mass spectrometers during the 1999 Atlanta supersite project. *J Geophys Res Atmos* 108:8424.
26. Thornton JA, et al. (2010) A large atomic chlorine source inferred from mid-continental reactive nitrogen chemistry. *Nature* 464:271–274.
27. VandenBoer TC, et al. (2013) Understanding the role of the ground surface in HONO vertical structure: High resolution vertical profiles during NACHTT-11. *J Geophys Res Atmos* 118:10155–10171.
28. EPA (2017) Emissions modeling platform, 2011 Version 6. Available at https://www.epa.gov/air-emissions-modeling/emissions-modeling-platforms. Accessed March 3, 2017.
29. EPA (2015) *Air pollutant emissions trends data*. Available at https://www.epa.gov/air-emissions-inventories/air-pollutant-emissions-trends-data. Accessed May 2, 2015.
30. Tai APK, et al. (2012) Meteorological modes of variability for fine particulate matter ($PM_{2.5}$) air quality in the United States: Implications for $PM_{2.5}$ sensitivity to climate change. *Atmos Chem Phys* 12:3131–3145.
31. Hanson PJ, Lindberg SE (1991) Dry deposition of reactive nitrogen compounds: A review of leaf, canopy and non-foliar measurements. *Atmos Environ A* 25:1615–1634.
32. Guo H, et al. (2017) Fine particle pH and gas-particle phase partitioning of inorganic species in Pasadena, California, during the 2010 CalNex campaign. *Atmos Chem Phys* 17:5703–5719.
33. Canagaratna M, et al. (2007) Chemical and microphysical characterization of ambient aerosols with the aerodyne aerosol mass spectrometer. *Mass Spectrom Rev* 26:185–222.
34. Dunlea EJ, et al. (2009) Evolution of Asian aerosols during transpacific transport in INTEX-B. *Atmos Chem Phys* 9:7257–7287.
35. Kimmel JR, et al. (2011) Real-time aerosol mass spectrometry with millisecond resolution. *Int J Mass Spectrom* 303:15–26.
36. Solomon PA, et al. (2014) U.S. National $PM_{2.5}$ chemical speciation monitoring networks-CSN and IMPROVE: Description of networks. *J Air Waste Manag Assoc* 64:1410–1438.
37. EPA (2017) Clean Air Status and Trends (CASTNET). Available at https://www.epa.gov/castnet. Accessed October 5, 2017.
38. Reinecker M, et al. (2008) The GEOS-5 data assimilation system-documentation of versions 5.0. 1, 5.1. 0, NASA Technical Report TM-2007. Available at https://gmao.gsfc.nasa.gov/pubs/docs/Rienecker369.pdf. Accessed August 15, 2016.
39. Travis KR, et al. (2016) Why do models overestimate surface ozone in the Southeast United States? *Atmos Chem Phys* 16:13561–13577.
40. EPA (2017) *Air markets program data*. Available at https://ampd.epa.gov/ampd/. Accessed March 3, 2017.